Adaptive Air Charge Estimation for Turbocharged Diesel Engines without Exhaust Gas Recirculation*

Ove F. Storset[1], Anna G. Stefanopoulou[2†] and Roy Smith[3]

[1,3]University of California Santa Barbara, CA 93106

[2]University of Michigan, Ann Arbor, MI 48109

September 15, 2003

Abstract

The paper presents an adaptive observer for in-cylinder air charge estimation for turbocharged diesel engines without exhaust gas recirculation (EGR). We assess the observability of the mean value engine model when the intake manifold pressure and the compressor flow are measured, and the performance of the observer is compared to existing schemes analytically and with limited simulations. Specifically, it is shown that the designed observer performs better than the conventional schemes during fast step changes in engine fueling level, eventhough it uses a simple but time varying parameterization of the volumetric efficiency. Furthermore, the estimate is less sensitive to changes in engine parameters than the existing schemes.

*Support for Storset and Stefanopoulou is provided by the National Science Foundation under contract NSF-ECS-0049025 and Ford Motor Company through a 2001 University Research Project; Smith is supported by the National Science Foundation under contract NSF-ECS-9978562.

†Corresponding author: annastef@umich.edu, TEL: +1 (734) 615-8461 FAX: +1 (734) 764-4256

1 Introduction

Fuel economy benefits obtained by turbocharged (TC) diesel engines render them common practice for the vast majority of medium and heavy duty commercial vehicles and are often met in passenger vehicles. Reduction of smoke emission, particulates, and nitrogen oxides are the challenges that the powertrain controller needs to address to make diesel-based propulsion environmentally friendly. Diesel engines operate at lean air/fuel mixtures with typical values 40:1 for diesel engines in contrast to 14.6:1 for conventional gasoline engines. To avoid generation of visible smoke and particulates the air-to-fuel ratio (AFR) needs to be higher than a critical value called "smoke limit" ($\text{AFR}_{sl} \approx 25$) as shown in Figure 1.

To maintain the AFR above the visible smoke limit, the vehicle controller estimates the cylinder air charge and limits the amount of fuel injected into the cylinders when $\text{AFR}<\text{AFR}_{sl}$. The estimation task here is more challenging than in throttled engines due to the transient behavior of the exhaust manifold pressure. The challenge arises from the fact that the volumetric efficiency that is the basis of cylinder air charge in all internal combustion engines depends on exhaust manifold pressure. In throttled and port fuel injection (PFI) engines with well designed exhaust manifold and tailpipe the exhaust manifold pressure follows the intake manifold pressure, so it can be eliminated from the volumetric efficiency as redundant variable.

In turbocharged Diesel engines the exhaust manifold pressure cannot be neglected from the volumetric efficiency because it has a distinct behavior from the intake manifold during transients. In engines equipped with Variable geometry turbocharging (VGT), flow assist mechanisms, and wastegating the interactions between the intake and exhaust subsystems increase even more and introduce significant transient phenomena. Due to these interactions with the exhaust manifold, the traditional steady-state, mean-value air-flow regression or volumetric efficiency that is solely based on measured intake manifold conditions is not sufficient for the transient air charge estimation of a turbocharged diesel engine.

Furthermore, air-to-fuel ratio cannot be easily measured in the lean and relatively cold diesel feedgas (or tailpipe) emissions. The task of lean air-to-fuel ratio measurement in diesel exhaust using a linear exhaust gas oxygen (UEGO) sensor is harder than the AFR measurement in the exhaust of gasoline engines (port injection [1], or direct injection [2]). Last, but not least, air charge estimation is very difficult during large exhaust gas

recirculation (EGR) introduced to reduce oxides of nitrogen [3, 4].

In this paper we address the air charge estimation problem **without EGR** by using adaptive observers and by measuring variables in the intake manifold. An adaptive observer for the air charge estimation of a direct injections spark ignition (DISI) engine is shown in [2]. The authors, however use an UEGO sensor in addition to other intake manifold measurements. They also propose the adaptation of a multiplicative factor in volumetric efficiency when EGR is set to zero. Air charge estimation has been achieved for non-zero EGR assuming extensive engine mapping [4], or measurements of exhaust manifold variables [5]. Recently in [6, 7], the authors show for the case study of a throttled SI engine that an adaptive observer of the air charge can achieve better steady state results even during engine aging or partially unknown volumetric efficiency maps. Finally, an observer for cylinder air flow in turbocharged diesel engine with wastegate has been designed and experimentally demonstrated in [8]. The work here is based on a time varying parametrization of volumetric efficiency that enables transient (instead of steady state) adaptation and accounting for the charge dependency on the exhaust manifold pressure. The observer designed in this paper provides better estimates during fuel transients than existing production schemes. The presented approach is less sensitive to modelling errors and aging than conventional methods. Unfortunately the proposed scheme cannot be directly extended to engines with EGR due to the additional complexity that EGR introduces by connecting the thermodynamic states of the intake and exhaust manifolds. Despite this significant limitation, the proposed scheme can potentially help reduce smoke emissions of old technology diesel engines, i.e., engines without EGR, that currently power the majority of land and marine transportation vehicles around the world.

We start in Section 2 by summarizing the general notation, whereas, the complete nomenclature is shown in Appendix C. In Section 3 we present the mean value model used to approximate the intake manifold dynamics together with a brief discussion of measurements and the limitations of the existing air charge estimation schemes. In Section 4 our methodology for estimating the air charge is outlined. We analyze observability of the mean value model in Section 5, and continue presenting the air charge estimation schemes in Section 6 with formal proof. One simulation example of its performance compared to existing schemes is provided in Section 7 to illustrate the differences between the algorithms during a simple fuel step change. The simulation is performed

on an engine model developed in [9] and used in several control and estimation studies [4, 10, 11]. We conclude the paper with a discussion of the algorithm limitations and range of applicability.

2 Notation

In the sequel, $\bar{(\cdot)}$ denotes a measured variable, or a variable constructed from measurements only, so that $\bar{x}$ is the measurement of x. The notation $\hat{(\cdot)}$ is used for estimated variables and the $\tilde{(\cdot)}$ is used for the error in the estimated variables.

Masses are denoted with m, mass flows with W, pressure with p, efficiencies with η, volumes with V, and temperatures with T. Mass flows will have two indices, W_{kl}, where "k" represents the origin of the flow and "l" is the destination. The following indices are used: "c" represents the compressor outlet, "i" the intercooler outlet, "1" the intake manifold, "a" ambient conditions, "e" the engine, "cyl" the cylinder, and "f" is fuel (see also Figure 2). The variable N denotes the engine rotational speed whereas ω_{tc} denotes the turbocharger rotational speed, both in revolutions per minute (rpm). A complete list of the variables is in Appendix C.

The set of positive real numbers excluding zero is denoted by $\mathbb{R}_+$, $\dot{x}$ denotes $\frac{d}{dt}x$, and $\mathcal{P}^n(x)$ is a n-th order polynomial in x. The operator $[Hu](t, N)$ denotes the output $y = c(N(t))x + d(N(t))u$ with $\dot{x} = a(N(t))x + b(N(t))u$. For convenience, the dependency on the time varying signal $N(t)$ will be omitted so that $[Hu](t) = [Hu](t, N)$. Similarly, we will omit the time dependence on signals so that $u = u(t)$, $N = N(t)$, etc.

3 Mean value model

The intake manifold dynamics are approximated using mean value modelling which disregards the engine events and the inertia of the gas. The flow through the engine is then continuous, and transportation delays are neglected. The engine is then approximated as a "continuous flow device" such as a pump.

This model is clearly not valid for short time intervals, but it has good accuracy on time scales slightly larger than an engine cycle [12, 13, 14]. The energy balance (Eq. (1)) and mass balance (Eq. (2)) in the intake manifold given adiabatic conditions result in the state equation for pressure, p_1, and mass, m_1, respectively. They are

related with the intake manifold temperature, T_1, through the ideal gas law (3):

$$\dot{p}_1 = \kappa k_1^2 \left(W_{c1} T_i - W_{1e} T_1 \right) \tag{1}$$

$$\dot{m}_1 = W_{c1} - W_{1e} \tag{2}$$

$$T_1 = \frac{1}{k_1^2} \frac{p_1}{m_1}, \quad k_1 = \sqrt{\frac{R_1}{V_1}}, \tag{3}$$

where V_1 is the volume of the intake manifold, κ is the ratio of specific heats, and R_1 is the gas constant for air. Note that the intercooler temperature, T_i, varies with compressor and intercooler efficiencies and is different from T_1 during transients. Thus the rate of change of pressure is, in general, different from the rate of change of mass. The fact that mass and pressure are independent during transients is usually neglected in conventional estimation schemes where T_i and T_1 are assumed equal and constant in an isothermal assumption. During isothermal conditions the two state equations (1)-(2) collapse to one (mass is proportional to pressure).

Note also that the we assume that the volume within and between the intercooler and the compressor is very small. This assumption has two important implications. First, the compressor downstream pressure, p_c, is a static function of the intake manifold pressure $p_c = p_1/\eta_p$. The static function corresponds to the pressure drop through the intercooler.

Second, the flow in the compressor is equal to the flow out of the intercooler (W_{c1}) even during transient conditions. Consequently, measuring the compressor inlet flow with a standard hot-wire anemometer device provides the instantaneous flow in the intake maniflod. The intercooler out-flow is in reality slightly different from the compressor in-flow due to leaks in the compressor and oil contamination from the turbocharger. Although these differences might become important after aging there is no concrete evidence of their significance and thus are ignored by current diesel engine management systems. In this work we acknowledge this additional challenge by formally proving that errors in W_{c1}, introduced by sensor drifts or modelling simplifications, does not destabilize the adaptive observer as most integrator-based adaptive schemes might do. Moreover, this error introduces a smaller estimation error in the proposed scheme than the traditional schemes during transients (see Sections 6 and 6.1). We finally, state that this error causes a bias in the estimated steady-state efficiency (see Section 6.1) similarly to the traditional air flow based cylinder charge estimation schemes.

In steady state the mean value flow into the engine W_{1e} equals the flow into the intake manifold, W_{c1}. The transient mean-value flow into the engine cylinders, W_{1e}, is given by the speed density equation [12]

$$W_{1e} = k_1^2 k_3 N m_1 \eta_v, \quad k_3 = \tfrac{V_d}{R_1 120}, \tag{4}$$

where V_d is the engine total displacement volume and η_v is the volumetric efficiency with respect to intake manifold conditions. The air charge trapped into the engine cylinders m_e during one engine cycle δ is given by

$$m_e = W_{1e}\delta, \quad \delta = 2\tfrac{60}{N}. \tag{5}$$

The estimation of the air charge is, thus, dependent on accurate estimation of the transient mean-value air flow in all the cylinders, $\hat{W}_{1e}$.

3.1 Volumetric efficiency

The volumetric efficiency is typically in the range $\frac{1}{2}$ to 1 for diesel engines. It is independent of the cylinder size, and it is a measurement of engine performance as an air pumping device. It is defined in Taylor [15] as : "The mass of fresh mixture which passes into the cylinder in one suction stroke, divided by the mass of the mixture which would fill the piston displacement at inlet density". Intuitively, it is the averaged fraction of in-cylinder mass density to mass density in the intake manifold, where the averaging is taken over one engine cycle. More precisely,

$$\eta_v(t) = \frac{\frac{1}{V_d}\int_{t-\delta}^{t} W_{1e}^{'}(\tau)\, d\tau}{\frac{1}{V_1}\frac{1}{\delta}\int_{t-\delta}^{t} m_1(\tau) d\tau}, \tag{6}$$

where W_{1e}' is the instantaneous flow into the engine, whereas W_{1e} is the averaged quantity. The volumetric efficiency can be derived analytically from ideal engine cycles as in Ferguson, p. 254 [16], Taylor, p. 160 [15], or Heywood [12], where it is computed from an intake event with valve overlap as

$$\eta_v = \left(\frac{1}{1+\frac{\Delta T}{T_1}}\right)\left(\frac{r-\frac{p_2}{p_1}}{\kappa\,(r-1)} + \frac{\kappa-1}{\kappa}\alpha\right), \tag{7}$$

where ΔT is the mean temperature rise of the intake gas during the intake stroke, m_{ol} is the mass of the exhaust gas being let into the cylinder during valve overlap, r is the compression ratio, and κ is the ratio of specific heats.

The variable α is defined as

$$\alpha := \frac{1}{p_1 V_d} \int_{\text{intake stroke}} p_{cyl}\ dV_{cyl}, \tag{8}$$

where p_{cyl} is the in-cylinder pressure and V_{cyl} is the transversed cylinder volume.

Due to the fact that the mean-value of the exhaust manifold pressure, p_2 follows the mean-value of the intake manifold pressure p_1, in throttled engines without turbocharger the dependency of η_v on $\frac{p_2}{p_1}$ is simplified and replaced with the corresponding dependency on p_1:

$$\eta_v = \eta_v(N, T_1, \frac{p_2}{p_1}) \approx \eta_v^{thr}(N, T_1, p_1). \tag{9}$$

This simplification has been shown accurate to 3% in [17] by Hendricks et. al.

This simplification, however, is not as accurate in diesel engines. In particular, the volumetric efficiency is more complex and is directly influenced by p_2 for several reasons. First, in diesel engines torque is controlled by varying the fueling level which affects p_2 very rapidly, consequently $\frac{p_2}{p_1}$ varies significantly during transients when p_2 does not follow p_1. Second, the unthrottled operation of diesel engines allows higher volumetric efficiency, where the filling and emptying dynamics are more sensitive to changes in p_1 and p_2. In turbocharged engines the intake and exhaust manifold pressures have a greater range so that $\frac{p_2}{p_1}$ varies more than in conventional engines [18]. Last but no least, in the case of a variable nozzle turbocharger (VNT), the exhaust manifold pressure is influenced by the opening of the turbine nozzles which consequently affects the volumetric efficiency through changes in p_2 (see [2]). These phenomena cause η_v of diesel engines to have a transient characterization different from its steady state behavior as shown in Figure 6 [15].

A parameterization of η_v, more appropriate for TC diesel engines suggested by dimensional analysis in [15], and applied in [19] is:

$$\eta_v = \eta_\rho(\tfrac{p_2}{p_1})\eta_z(N, \sqrt{T_1}), \tag{10}$$

where η_ρ accounts for the losses in the filling and emptying due to different pressures in the exhaust and intake manifold. The term η_z accounts for the dependency of the volumetric efficiency on the velocity of the air entering the cylinder which depends on N through the piston speed and $\sqrt{T_1}$ through the velocity of sound in the intake manifold (Mach number). The effect of temperature can be factored out of the volumetric efficiency and captured

in a great extend by the intake manifold mass ($m_1 = p_1/(k_1^2 T_1)$) that proceeds η_v in Equ. (4). Thus η_v depends on p_1, p_2, N. However, this parameterization requires a p_2 measurement which is not easy to obtain due to the adverse conditions in the exhaust manifold. Although a p_2-sensor has been assumed in recent diesel control methodologies [5, 11], the sensor technology is not mature yet to be considered for production. To circumvent the p_2 based parameterization, we will assume that the volumetric efficiency depend on N and a time varying parameter $\theta(t)$ that needs to be identified so that

$$\eta_v(t) = \mathcal{P}_\rho(N(t))\theta(t), \tag{11}$$

where $\mathcal{P}_\rho(N) > 0$ is a polynomial in N that accounts for the pumping rate's dependency on engine speed. $\theta(t)$ is an unknown **time varying coefficient** that accounts for all the other phenomena mentioned.

The model (1)-(2) with this parameterization becomes:

$$\dot{p}_1 = -\kappa k_1^2 k_3 N \mathcal{P}_\rho(N)\theta p_1 + \kappa k_1^2 W_{c1} T_i \tag{12}$$

$$\dot{m}_1 = -k_1^2 k_3 N \mathcal{P}_\rho(N)\theta m_1 + W_{c1}. \tag{13}$$

We will assume a fast and accurate engine speed sensor $\bar{N} = N$. A hot wire anemometer is used for the measurement of the mass air flow into the intake manifold, $\bar{W}_{c1}$. A pressure transducer is used for the measurement of the intake manifold pressure $\bar{p}_1 = p_1 + \Delta p_1$, where Δp_1 represents the pressure flunctuations from the cylinder-to-cylinder breathing. It is important to estimate the deliterious effects of these unmodeled dynamics to the identified parameter $\theta(t)$.

3.2 Traditional air charge estimation

In throttled spark ignited engines air charge estimation is traditionally achieved based on a mass air flow (MAF) sensor for the air flow into the intake manifold, $\bar{W}_{c1}$. For simplicity we call this scheme as **MAF**-based air charge estimation. This scheme uses a map engine's steady state pumping rate $\mathcal{P}_{Wf}(N, W_f)$ based on engine speed and fuel charge injected W_f or $\mathcal{P}_W(N, p_1, T_1)$ based on intake manifold pressure and temperature as shown in Eq. (9). In modern diesel engines where a wastegate or other active turbocharging devices are used (typically to allow manipulation of the intake manifold pressure independently of the fueling) the mapping $\mathcal{P}_W(N, p_1, T_1)$

is preferred. The temperature of air entering the intake manifold is assumed equal to the intake manifold temperature T_1, and $\hat{p}_1$ is estimated in an open loop observer as,

$$\dot{\hat{p}}_1 = \kappa k_1^2 T_1(-\mathcal{P}_W(N, \hat{p}_1, \bar{T}_1) + \bar{W}_{c1}) \tag{14}$$

$$\hat{W}_{1e} = \mathcal{P}_W(N, \hat{p}_1, \bar{T}_1), \tag{15}$$

where $\bar{T}_1$ is assumed constant or measured with a low bandwidth device [20]. In steady state the error $\tilde{W}_{1e} := W_{1e} - \hat{W}_{1e}$ is given by $\tilde{W}_{1e} = \tilde{W}_{c1}$ which is small when the measurement error $\tilde{W}_{c1} := W_{c1} - \bar{W}_{c1}$ is small; however, this is not always the case.

Another traditional air charge estimation algorithm is the so called **speed density** (or "MAP"-based) scheme. In this scheme a measurement of p_1 is used to calculate the approximate intake manifold density $\rho := \frac{m_1}{V_1} = \frac{1}{V_1 k_1^2}\frac{p_1}{T_1}$ where T_1 is assumed constant or measured with a low bandwidth device. The volumetric efficiency is approximated by the steady state engine pumping rate, $\mathcal{P}_v(N, p_1)$ (9), so that W_{1e} is approximated as

$$W_{1e} = k_1^2 k_3 N m_1 \eta_v = k_3 N \frac{p_1}{T_1}\eta_v \tag{16}$$

$$\approx k_3 N \frac{p_1}{T_1}\mathcal{P}_v(N, p_1) (= \mathcal{P}_w(N, p_1, T_1))$$

$$\hat{W}_{1e} = \mathcal{P}_w(N, \bar{p}_1, \bar{T}_1) \tag{17}$$

The speed density scheme relies on the accuracy of the $\mathcal{P}_v\,(N, p_1)$ map and has a steady state error if the map is incorrect.

Both schemes can be quite precise on large time scales in naturally aspirated gasoline engines where a throttle is used to manipulate manifold pressure, and consequently the cylinder air charge, thereby controlling the brake torque [17]. In this case, the exhaust pressure, p_2, follows the changes in p_1 even during transients so the volumetric efficiency does not depend strongly on p_2, and the map $\mathcal{P}_v(N, p_1)$ is a good approximation of η_v.

Since neither of the traditional schemes accounts for the dynamic properties of η_v, there is a significant error in the η_v estimate during changes in the fueling level in TC diesel engines, and thus a parameterization of η_v based on p_1 only cannot capture the transient behavior of the engine air flow. Unfortunately, this happens exactly when a reliable air charge estimate is needed to maintain an acceptable transient air-to-fuel ratio, and to avoid visible smoke emissions.

4 Proposed solution

To estimate the air charge and the cylinder air flow, W_{1e}, more precisely, there must be more information about the variations in η_v in addition to a satisfactory m_1 estimate. We follow the adaptive observer technique first presented in [21] and schematically shown in Fig. 3. Specifically, we parameterize the volumetric efficiency by $\eta_v(t) = \mathcal{P}_\rho(N)\theta(t)$ using (11) and attempt to approximately track the unknown coefficient $\theta(t)$ through an identification scheme relying on variables estimated by an observer as shown in Figure 3. Similar observer techniques with on-line estimation of η_v using measurement of p_1 and W_{thr} (throttled mass flow) in a throttled SI engine were shown recently in [6].

In this paper we rigorously prove that by using known signals (measurements y and inputs u) $[y, u] = [p_1, W_{c1}, N]$ and by constructing $\bar{T}_i$ using these known signals (shown in Appendix A), we achieve closed loop tracking of $\theta(t)$. The intake manifold mass m_1 is then estimated open loop because it is shown to be unobservable. We show via simulations that the adaptive observer can capture the fast changes in the volumetric efficiency and achieve transient estimation of the in-cylinder air flow $\hat{W}_{1e}$ and thus the engine air charge $\hat{m}_e$.

5 Observability of the model

We start with a few remarks on nonlinear observability. If we assume that we have perfect knowledge of the plant, the inputs and the outputs except its present state, the issue of observability for a stable plant addresses whether it is possible to create an observer whose state estimate converges faster to the actual state than the plants dynamics. Observability for nonlinear systems can be defined in terms of indistinguishable states introduced in [22] and more tractable local concepts presented in [23]. However, for nonlinear systems, observability is in general not enough to be able to design a closed loop observer. The additional condition of the plant being uniformly observable (UO) guarantees the existence of an observer for the system, but the structure of the observer is in general not known even if the plant is UO.

Even if we know the volumetric efficiency (perfect knowledge of plant) to estimate $\hat{W}_{1e}$ we need to produce an estimate of m_1 since it cannot be measured directly. If the input $u^T = [W_{c1}, T_i, N]$ is known, observability of m_1

can then be assessed from p_1 measurements assuming correct system equations, (12)-(13), and perfect knowledge of η_v (that will be achieved through the closed loop identifier in the following section). Equations (12)-(13) and (3) can be written

$$\begin{bmatrix} \dot{p}_1 \\ \dot{m}_1 \end{bmatrix} = \begin{bmatrix} -\kappa k_1^2 k_3 N(t)\eta_v(t)p_1 + \kappa k_1^2 W_{c1} T_i \\ -k_1^2 k_3 N(t)\eta_v(t)m_1 + W_{c1} \end{bmatrix} \tag{18}$$

$$p_1 = [1\ 0]\, x = Cx \tag{19}$$

where $x^T = [p_1, m_1]$ is the state and $y = p_1$ is the output measurement. For any input $u'^T = [W_{c1}T_i, W_{c1}]$ and with $N(t)$ known variable, the state equation (18) can be viewed as a linear time varying system

$$\begin{bmatrix} \dot{p}_1 \\ \dot{m}_1 \end{bmatrix} = \begin{bmatrix} -\kappa a(t) & 0 \\ 0 & -a(t) \end{bmatrix} \begin{bmatrix} p_1 \\ m_1 \end{bmatrix} + \begin{bmatrix} \kappa k_1^2 & 0 \\ 0 & 1 \end{bmatrix} \begin{bmatrix} W_{c1}T_i \\ W_{c1} \end{bmatrix} \tag{20}$$

$$a(t) = k_1^2 k_3 N(t)\eta_v(t)$$

with a linear output equation $y = p_1 = Cx$ (19). The output equation (19) does not contain m_1, and the rate of change of the two states is decoupled in (20). All pairs of states $([p_1(t_0), m_1(t_0)]^T, [p_1(t_0), m_1'(t_0)]^T)$, such that $m_1(t_0) \neq m_1'(t_0)$ are indistinguishable so the m_1 is unobservable from p_1.

If we consider instead (or in addition) to pressure p_1 a fast temperature measurement $y = T_1 = \frac{1}{k_1^2}\frac{p_1}{m_1}$ the system is observable. This indicates that if fast temperature sensors were available one can design a closed loop estimator for m_1. Unfortunately, even if fast temperature sensors are available, there are many challenges associated with the potential differences between the temperature and pressure sensor dynamics in this scheme that are briefly discussed in [21].

6 Adaptive Observer Scheme

Since m_1 is unobservable from the measurements, it is not possible to make a closed loop observer of m_1, so we use the open loop observer for $\hat{m}_1$ and $\hat{W}_{1e}$ based on the identified parameter $\hat{\theta}(t)$ and the measured $\bar{W}_{c1}$ and $\bar{N} = N$ that is assumed free of errors.

$$\dot{\hat{m}}_1 = -k_1^2 k_3 N \mathcal{P}_\rho(N)\hat{\theta}\hat{m}_1 + \bar{W}_{c1} \tag{21}$$

$$\hat{W}_{1e} = k_1^2 k_3 N \mathcal{P}_\rho(N)\hat{\theta}\hat{m}_1, \tag{22}$$

The identification of $\hat{\theta}(t)$ follows. We assume that both $\bar{p}_1$ and $\bar{W}_{c1}$ are measured with possible errors, that $\bar{N} = N$, and that $\bar{T}_i$ is constructed as explained in Appendix A. We use the estimate of p_1:

$$\dot{\hat{p}}_1 = -\kappa k_1^2 k_3 N \mathcal{P}_\rho(N)\hat{\theta}\bar{p}_1 + \kappa k_1^2 \bar{W}_{c1}\bar{T}_i \tag{23}$$

$$+g_{p1}(\bar{p}_1 - \hat{p}_1), \quad g_{p1} > 0,$$

to create an identification error for the unknown parameter $\theta(t)$ based on the observer gain g_{p1} to be determined in the design process. The purpose of the feedback term, g_{p1}, in (23) is to prevent Δp_1 from destabilizing the adaptive scheme. Its purpose can heuristically be explained as making Δp_1 zero mean with respect to $\hat{p}_1$. This way the error, $\bar{p}_1 - \hat{p}_1$, which drives the adaptive law as shown below, does not contain a constant component from the disturbance Δp_1. Such constant disturbances can, when integrated in the observer and in the adaptive law, cause $\hat{\theta}$ to drift and obstruct convergence [24].

To make a reliable identification scheme for θ we have to find an identification error that is implementable based on measured signals and is linear in θ to guarantee convergence of $\tilde{\eta}_v$ to 0. This task is an art and requires a lot of experience with adaptive laws, so we cover all the details as a tutorial in the following equations. As a road map, we briefly state that the implementable identification error is given by Eq. (36) and based on the regressor in Eq. (26).

Manipulating (12) gives

$$\left[\frac{d}{d\tau}p_1\right](t) - \kappa k_1^2 W_{c1}(t)T_i(t) \tag{24}$$

$$= -\kappa k_1^2 k_3 N(t)\mathcal{P}_\rho(N(t))p_1(t)\theta(t).$$

Since (24) is not proper and therefore not realizable, we filter both sides with the stable filter H_f as

$$\left[H_f \frac{d}{d\tau} p_1\right](t) - \left[H_f \kappa k_1^2 W_{c1} T_i\right](t) \tag{25}$$
$$= -\left[H_f \kappa k_1^2 k_3 N \mathcal{P}_\rho(N) p_1 \theta\right](t).$$

We define $[\phi\theta](t) := -\left[H_f \kappa k_1^2 k_3 N \mathcal{P}_\rho(N) p_1 \theta\right](t) = -\left[H_f G_{pN} p_1 \theta\right](t)$. Omitting the time dependence in the signals and using the measured pressure $\bar{p}_1 = p_1 + \Delta p_1$ we also define the regressor:

$$\bar{\phi}(t) = -\left[H_f G_{pN} \bar{p}_1\right] \tag{26}$$

which is always nonzero and therefore persistently exciting (PE). We then define the signal

$$z := \left[\bar{\phi}\theta\right] := -\left[H_f G_{pN} \bar{p}_1 \theta\right] \tag{27}$$
$$= -\left[H_f G_{pN}(p_1 + \Delta p_1)\theta\right] = -\left[H_f G_{pN} p_1 \theta\right] - \left[H_f G_{pN} \Delta p_1 \theta\right]$$
$$= \left[H_{df} p_1\right] - \left[H_f G_w W_{c1} T_i\right] - \left[H_f G_{pN} \Delta p_1 \theta\right] \tag{28}$$

where, $[H_{df}](t) = \left[H_f \frac{d}{d\tau}\right](t)$, $G_{pN} := \kappa k_1^2 k_3 N \mathcal{P}_\rho(N)$ and $G_w := \kappa k_1^2$. Since the frequency of the disturbance Δp_1 is varying with $N(t)$ it is beneficial to make the cutoff frequency of the filters H_{df} and H_f dependent on $N(t)$:

$$[H_f u_f](t) = x_f, \text{ with } \dot{x}_f = -k_\omega N x_f - k_\omega N u_f \tag{29}$$

$$[H_{df} u_{df}](t) = x_{df} + k_\omega N u_{df} \text{ with } \dot{x}_{df} = -k_\omega N x_{df} - k_\omega^2 N^2 u_{df}. \tag{30}$$

Let the estimated signal

$$\hat{z} := \left[\bar{\phi}\hat{\theta}\right] := -\left[H_f G_{pN} \bar{p}_1 \hat{\theta}\right] \tag{31}$$
$$= \left[H_{df} \hat{p}_1\right] - \left[H_f G_w \bar{W}_{c1} \bar{T}_i\right] - \left[H_f g_{p_1}(\bar{p}_1 - \hat{p}_1)\right] \tag{32}$$
$$= \left[H_{df} \hat{p}_1\right] - \left[H_f g_{p_1} \tilde{p}_1\right] - \left[H_f G_w \bar{W}_{c1} \bar{T}_i\right] - \left[H_f g_{p_1} \Delta p_1\right]$$

From Eq. 27 and 31 and the regressor 26 we define the identification error:

$$\epsilon(t) := z(t) - \hat{z}(t) = \left[\bar{\phi}\theta\right](t) - \left[\bar{\phi}\hat{\theta}\right](t) = -\left[H_f G_{pN} \bar{p}_1 \tilde{\theta}\right](t)$$
$$= \bar{\phi}(t)\tilde{\theta}(t) - \left[H_s \bar{\phi}(\tau)\dot{\tilde{\theta}}(\tau)\right](t) = \bar{\phi}(t)\tilde{\theta}(t) - \varepsilon_s, \tag{33}$$

which is linear in the parameter error $\tilde{\theta}$. The term ε_s originates from pulling $\tilde{\theta}$ out of the filter H_f using Morse's swapping lemma [25] for the first term in the filter operator H_f as

$$\left[H_f\tilde{\theta}\psi\right](t) = \tilde{\theta}(t)\left[H_f\psi\right](t) - \left[H_s\left[H_f\psi\right](\tau)\dot{\tilde{\theta}}(\tau)\right](t), \quad \left[H_f\psi\right](t) = \bar{\phi}(t)$$

where the filter H_s is given by:

$$\left[H_s u_s\right](t) := x_s, \quad \text{with} \quad \dot{x}_s = -k_\omega N x_s + u_s \tag{34}$$

The identification error $\epsilon(t)$ using Eq. 28 and 32 can be written with measured and estimated variables as

$$\begin{aligned}
\epsilon(t) &:= z(t) - \hat{z}(t) \\
&= [H_{df}p_1] - [H_f G_w W_{c1} T_i] - [H_f G_{pN}\Delta p_1 \theta] - [H_{df}\hat{p}_1] + \left[H_f G_w \bar{W}_{c1}\bar{T}_i\right] + [H_f g_{p_1}(\bar{p}_1 - \hat{p}_1)] \\
&= [H_{df}\left(\bar{p}_1 - \hat{p}_1\right)] + [H_f g_{p1}\left(\bar{p}_1 - \hat{p}_1\right)] + [H_{df}\Delta p_1] - [H_f G_{pN}\theta\Delta p_1] - \left[H_f G_w \widetilde{W_{c1}T_i}\right] \\
&= [\left(H_{df} + g_{p1}H_f\right)\left(\bar{p}_1 - \hat{p}_1\right)] + [H_{df}\Delta p_1] - [H_f G_{pN}\theta\Delta p_1] - \left[H_f G_w \widetilde{W_{c1}T_i}\right],
\end{aligned} \tag{35}$$

where $\widetilde{W_{c1}T_i} = W_{c1}T_i - \bar{W}_{c1}\bar{T}_i$. Since no information is available for Δp_1, nor for $\widetilde{W_{c1}T_i}$, these terms cannot participate in the implementation of the on-line identifier, thus they cause a bias in the estimate of $\hat{\theta}$ that we continue to keep track in the proof of the identifier convergence. We implement the identification error

$$\bar{\epsilon}(t) = [(H_{df} + g_{p1}H_f)(\bar{p}_1 - \hat{p}_1)](t) = [H_{dgf}(\bar{p}_1 - \hat{p}_1)](t) \tag{36}$$

which is the first term in (35), where

$$\left[H_{dgf}u_{dgf}\right](t) = x_{dgf} + k_\omega N u_{dgf} \quad \text{with} \quad \dot{x}_{dgf} = -k_\omega N x_{dgf} + k_\omega N(g_{p1} - k_\omega N)u_{dgf}. \tag{37}$$

The updating law

$$\dot{\hat{\theta}} = \begin{cases} (\Gamma + P)\bar{\phi}(t)\bar{\epsilon}(t) & \hat{\eta}_v = \mathcal{P}_\rho(N)\hat{\theta} \in \mathcal{S}_\eta \\ 0 & \hat{\eta}_v = \mathcal{P}_\rho(N)\hat{\theta} \notin \mathcal{S}_\eta \end{cases}, \tag{38}$$

is the combination of the traditional gradient and least squares with projection and covariance resetting at time t_r. $\Gamma > 0$, and the time varying P is given by:

$$\dot{P} = \begin{cases} -P^2\bar{\phi}^2 & \hat{\eta}_v = \mathcal{P}_\rho(N)\hat{\theta} \in \mathcal{S}_\eta \\ 0 & \hat{\eta}_v = \mathcal{P}_\rho(N)\hat{\theta} \notin \mathcal{S}_\eta \end{cases}, \tag{39}$$

where $P(t)$ is reset to $P(t_r) > 0$ when the fueling level of the engine changes faster than some chosen threshold.

Ideally, the least squares adaptive gain reset value $P(t_r)$ should be made a function of engine speed and fueling level, $P(t_r) = f(N, W_f)$, to assure the same rate of convergence of $\hat{\theta}$ at all operating points of the engine. This gives faster adaptation when the volumetric efficiency is expected to change, whereas the gradient algorithm assures a small identification error in $\hat{\eta}_v$ when it changes slowly. Otherwise, the adaptation might be very slow at low N and W_f, and oscillatory at high values of N, and W_f.

Increased value of the adaptive gain, $\Gamma + P$, gives more measurement noise from $\bar{p}_1$ in $\hat{\theta}$. The filter coefficient k_ω has a similar effect on the convergence of $\hat{\theta}$. When it is set too high, it creates more noise in $\hat{\theta}$, and when it is set too low it results in slower convergence of $\hat{\theta}$.

To assure that $\hat{\eta}_v \in \mathcal{S}_\eta$, the update law utilizes projection as in [26]. Notice that the projection set $\mathcal{S}_\eta$ defines the set $\mathcal{S}_\theta(t)$ that varies as $\mathcal{P}_\rho(N(t))$ varies with time. See Appendix B.1 for definitions of $\mathcal{S}_\theta$, $\mathcal{D}$ and $\mathcal{U}$.

Define the following conditions:

Condition 1 *$x \in \mathcal{D}$ and $u \in \mathcal{U}$ $\forall t \geq t_0$ where $\mathcal{D}$ and $\mathcal{U}$ are compact.*

Condition 2 *$\Delta p_1 = 0$ and $\tilde{W}_{c1} = 0$ $\forall t$, and $\tilde{T}_i$, θ and N are independent of time.*

Condition 3 *$\tilde{T}_i = 0$ $\forall t$.*

Theorem: The given adaptive observer (21) - (23) with the identification error (36) utilizing the filter (29) and (37) with the combined least squares and gradient updating law (38) and (39) with parameter projection has the following properties:

Proposition 1 *Condition 1 implies $\hat{\theta}, \hat{p}_1, \hat{m}_1 \in \mathcal{L}_\infty$ (all signals are bounded).*

Proposition 2 *If further Condition 2 is satisfied $\tilde{W}_{1e} \to 0$ exponentially as $t \to \infty$.*

Proposition 3 *If Conditions 1-3 are satisfied we additionally have that $\tilde{\theta}$, $\tilde{\eta}_v \to 0$ exponentially as $t \to \infty$.*

The proofs are given in Appendix B.

6.1 Effect of measurement errors

The pressure fluctuations due to the cylinder pumping are present in $\bar{p}_1$ as Δp_1. With this disturbance the estimation error $\tilde{W}_{1e}$ belongs to a small neighborhood of the origin (see Figure 6). Notice that $\tilde{W}_{1e}$ is large when the input $u = [\widetilde{W_{c1}T_i}, \Delta p_1, \dot{\theta}]$ to the error system (57) is large, in particular, when $\dot{\theta}$ changes fast.

A constant error between the actual T_i and measured (or constructed) $\bar{T}_i$, biases $\hat{\eta}_v$, but $\tilde{m}_1$ is also nonzero and counteracts $\tilde{\eta}_v$ in the output equation (22) so that in steady state

$$\tilde{\eta}_v = \eta_v \frac{\tilde{T}_i}{T_i}, \quad \tilde{m}_1 = m_{1E} \frac{\tilde{T}_i}{\tilde{T}_i - T_i}, \quad \tilde{W}_{1e} = 0, \tag{40}$$

where m_{1E} is the equilibrium value of m_1. However, a time varying $\tilde{T}_i$ causes an error in $\hat{W}_{1e}$ because the time constant of (21), $k_1^2 k_3 N \mathcal{P}_\rho(N)\hat{\theta}$, determines the rate with which $\tilde{m}_1$ counteracts the error imposed by $\tilde{T}_i$ in $\tilde{\eta}_v$.

Notice that the air charge estimate $\hat{W}_{1e}$ will converge to the correct value even if there is a steady state error in $\bar{T}_i$. An efficient and well designed intercooler ensures small variation in T_i. This approximation only serves to improve $\hat{W}_{1e}$ slightly when T_i is changing at its maximum rate. Therefore, our adaptive observer does not rely on constructing $\bar{T}_i$ as in Appendix A, it is merely included to improve accuracy if desirable. In fact, in the estimation algorithm $\bar{T}_i$ could be taken to be a constant with only minor deterioration in the air charge estimate. However, the identification will not work if the input T_i is replaced by the state T_1 in the derivation of the algorithm as done in the "MAF"-based scheme in equation (14). Under these conditions the two states in Equ.(20) are redundant and their independent estimation is meaningless and potentially deleterious under numerical noise.

If there is a measurement error in W_{c1}, $\tilde{W}_{c1} \neq 0$, $\hat{\theta}$ is biased. In general, this bias gives a smaller error during transients than the traditional schemes in Section 3.2, but the steady state error is:

$$\tilde{\eta}_v = \eta_v \frac{\tilde{W}_{c1}}{W_{c1}}, \quad \tilde{m}_1 = 0, \quad \tilde{W}_{1e} = \tilde{W}_{c1}, \tag{41}$$

which is the same as the error in the "MAF"-based scheme (14).

7 Simulations

The proposed algorithm is here demonstrated with a simple simulation test during a fuel step change. All simulations are performed with a mean value model of a turbocharged 2.0 l diesel engine with variable geometry turbocharger and with an intercooler as documented in [9] and consequently used for many control studies in [10] and [11]. The fueling level is 5 kg/h, and has a positive step at time 0.2 s to 15 kg/h and a negative step back to 5 kg/h at t=0.7 s for constant engine speed starting at at 2500 rpm. Changes in fuel are the most critical transients because AFR has a big excursion and the traditional (p_1-based) volumetric efficiency model is not accurate during transients due to the p_2 dynamic behavior. Changes in engine speed need to be accommodated by parameter varying filters as in our adaptive scheme. For a realistic simulation we also change the load torque applied in the rotational dynamics of the combined vehicle-engine during the step change in fueling level. As one can see from Figure 4 a large step change in fuel needs to be followed with a VGT nozzle or wastegate opening so that the boost pressure stays within safe limits ($p_1 < 240$ kPa).

The various measurements p_1, N, and W_{c1} are obtained through sensors that have various time constants and can be represented with filters similar to Eq. 29. The measured pressure is given by:

$$\bar{p}_1 = H_{p1}(p_1 + \Delta p_1) \tag{42}$$

$$\Delta p_1(t) = (0.127324 - \left|\sin(\frac{2\pi}{60}N(t))\right|)0.0125p_1 \tag{43}$$

where the time constant of H_{p1} is 5 ms, and there is a 2.5% ripple in $\bar{p}_1$. The measured compressor flow is $\bar{W}_{c1} = H_{wc1}W_{c1}$ with a time constant of 20 ms. Engine speed is measured perfectly. The time constant for $\bar{T}_1$ is 1.0 s in the MAF and SD schemes. The most important states and estimated states are shown in Figure 5.

The volumetric efficiency of the model is

$$\eta_v = \mathcal{P}_m^3(N)(1 - 0.003(p_2' - p_1)) \tag{44}$$

$$\text{where, } \; p_2'(t) = p_2(t - \delta(t)) \tag{45}$$

with $\delta(t) = \frac{60}{N(t)}\frac{1}{2}$ and $\mathcal{P}_m^3(N)$ is a third order polynomial representing steady state pumping as a function of engine speed. Since p_2 is calculated instantaneously in the mean-value model (see [9]) based on an energy

equation similar to (1), a delay is necessary to capture Injection-to-Exhaust delay. Specifically, the exhaust manifold pressure at event k depends on the fuel and cylinder air charge of event $k-1$.

The pumping rate for the traditional (SD and MAF) schemes in Eq. (14)-(17) is

$$\hat{\eta}_v = \mathcal{P}_v(N, p_1) = ((\mathcal{P}_m^3(N) + 0.15)(1 - 0.003(p_{2mean} - p_1)) \tag{46}$$

where p_{2mean} is taken to be the average value of p_2 in the simulation. In other words, just for demonstration of the issues, $\mathcal{P}_v(N, p_1)$ has a large constant deviation of 15% from the one used in the simulation model.

In the proposed scheme the η_v parameterization is

$$\hat{\eta}_v = (\mathcal{P}_m^3(N) + 0.15)\hat{\theta} \tag{47}$$

so that the steady state pumping map has an error of 15% as in the MAF and Speed density schemes. The simulation parameters are: $k_\omega = 0.05$, $P(t_r) = 0.0002$, $\Gamma = 0.00004$, $g_{p1} = 1000$, $T_i = 200 + 1.04\bar{p}_1/p_a$ where $p_a = 101\ kPa$ in both the simulation model and the observer.

The speed density has a steady state error since there is a 15% error in the engine pumping map, as opposed to MAF and our observer which have no steady state error. The results for our observer are shown in Figure 6, and illustrates that our method better estimates the transient behavior of the air charge W_{1e}. Note that there is nothing particular about our demonstration choices of 15% error. More error in the η_v parametrization would cause larger larger bias in the SD scheme and slower convergence of the MAF scheme, whereas, it does not affect the proposed algorithm. Similarly, there is nothing specific to the polynomial $\mathcal{P}_m^3(N)$ we choose in our simulation and parameterization other than it has to fit the experimental data. Different characterizations will require tuning the gains of the proposed scheme.

8 Concluding Remarks and Algorithm Limitations

We propose an adaptive observer for in-cylinder charge estimation in diesel engines with no EGR. Rigorous proof and a simple simulation are showing that the proposed scheme performs better than the traditional MAF-based and MAP-based algorithms. One should not forget that if the intake manifold model we used for this observer is

not correct, it might not be possible to reconstruct the states accurately. Careful tuning and verification of the model constants κ, k_1 and k_3 should proceed the observer tuning process. Extra precaution is also recommended if this scheme is to be applied to an engine with a throttle or a Bernoulli orifice after the compressor.

The presence of EGR presents several challenges for air charge estimation and limits the applicability of our adaptive observer scheme. Most notable is that the air flow into the engine depends on the burnt gas fraction in the intake manifold F_1. Unfortunately, it is difficult to measure F_1 directly, but it may be estimated with an open-loop observer using the burnt gas fraction balance of the intake manifold as done in [4]. EGR also couples the intake and exhaust manifold filling dynamics. This coupling introduces an important term (the EGR flow multiplied with the EGR Cooler Temperature, $W_{egr}T_{ec}$) in the mass balance of the intake manifold. Typically this term is unknown during transients and it will contribute to the identification error ϵ, just as the measurement error of W_{c1}. This will bias the identified volumetric efficiency parameter $\hat{\theta}(t)$ significantly and obstruct convergence. Even if real-time measurement of the exhaust manifold pressure becomes available, the EGR flow can be calculated well only at steady-state using the orifice equations and steady-state maps for the EGR cooler temperature.

In summary, in the EGR case one can concentrate on schemes for steady-state (or slow-varying) adaptation of unknown engine parameters as in [7] and avoid elaborate modifications of the proposed transient identifier. The proposed adaptive observer can be employed in all old technology, i.e. without EGR, engines that still power the majority of the commercial trucks, ships, and locomotives around the world.

A Approximation for temperature of inflow to the intake manifold

In adaptive observer it is desirable to have an approximate air temperature of the inflow to the intake manifold, T_i. We seek to obtain an approximation of T_i based on measurements of p_1 and W_{c1} using available models of the turbocharger and intercooler.

The temperature out of the compressor is

$$T_c = T_a \left[1 + \frac{1}{\eta_c(\frac{p_1}{p_a}, \omega_{tc})} \left(\left(\frac{p_1/\eta_p}{p_a} \right)^{\frac{\kappa-1}{\kappa}} - 1 \right) \right], \tag{48}$$

where T_a and p_a are ambient temperature and pressure respectively, and ω_{tc} is turbocharger speed. The compressor efficiency, $\eta_c(p_1, \omega_{tc})$, is the ratio of isentropic temperature rise to the actual temperature rise across the compressor, and is used to compensate for the losses caused by other physical effects which are difficult to model (see [18, 9]). This model does not capture the heat storage effects of the compressor body, so the actual compressor temperature deviates from this. If an intercooler with air coolant is used, the temperature out of the intercooler, T_i, becomes

$$\begin{aligned} T_i &= T_a \left[1 + \frac{1}{\eta_c(\frac{p_1}{p_a}, \omega_{tc})} \left(\left(\frac{p_1/\eta_p}{p_a} \right)^{\frac{\kappa-1}{\kappa}} - 1 \right) (1 - \eta_i) \right] \\ &= T_a \gamma_{Tic}(\tfrac{p_1}{p_a}, \omega_{tc}, \eta_i), \end{aligned} \tag{49}$$

where the intercooler efficiency, η_i, can be treated as a constant or modeled as a function of the flow W_{c1} and/or vehicle speed.

The flow through the compressor, W_{c1}, is typically modelled with a map, $\gamma_{cm}(\frac{p_1}{p_a}, \omega_{tc})$, called the compressor mass flow parameter,

$$W_{c1}\left(p_1, \omega_{tc}, p_a, T_a\right) = \frac{p_a}{\sqrt{T_a}} \gamma_{cm}\left(\frac{p_1}{p_a}, \omega_{tc}\right), \tag{50}$$

and a typical shape of this map is given in Figure 7.

If the operating point $(\frac{p_1}{p_a}, \omega_{tc})$ is in the surge region, the compressor flow is unstable which may cause reverse flow. If the compressor flow reaches the speed of sound, chocking occurs; any further increase of ω_{tc} will not increase the flow. The steady state operating point $(\frac{p_1}{p_a}, \omega_{tc})_{ss}$ is determined by the steady state flow into the engine and the fueling level.

The maximum allowable intake manifold pressure limits the turbocharger speed, which in turn restricts the dynamic deviations of the steady state operating point, $(\frac{p_1}{p_a}, \omega_{tc})_{ss}$, away from the choking region. Surges can occur but only for short periods of time if we assume a reasonable engine controller. In this operating region the map $f_\gamma : (\frac{p_1}{p_a}, \omega_{tc}) \to \gamma_{cm}$ is one-to-one so that the function $f_\omega : (\frac{p_1}{p_a}, \gamma_{cm}) \to \omega_{tc}$ is well defined, and the turbocharger speed can be modeled as a function of the measurements p_1 and W_{c1} as

$$\omega_{tc} = f_\omega(\tfrac{p_1}{p_a}, \gamma_{cm}) = f_\omega(\tfrac{p_1}{p_a}, \tfrac{\sqrt{T_a}}{p_a} W_{c1}).$$

If we insert this expression into η_c we get.

$$\eta_c = \eta_c(\tfrac{p_1}{p_a}, \omega_{tc}) = \eta_c(\tfrac{p_1}{p_a}, f_\omega(\tfrac{p_1}{p_a}, \tfrac{\sqrt{T_a}}{p_a} W_{c1})),$$

and construct the compressor efficiency based on measurements of p_1, W_{c1}, p_a, T_a as

$$\hat{\eta}_c = \hat{\eta}_c(\bar{p}_1, \bar{W}_{c1}, \bar{p}_a, \bar{T}_a) = \eta_c(\tfrac{\bar{p}_1}{p_a}, f_\omega(\tfrac{\bar{p}_1}{p_a}, \tfrac{\sqrt{\bar{T}_a}}{p_a} W_{c1})).$$

The approximation for T_i then becomes

$$\begin{aligned} \bar{T}_i &= \bar{T}_a \left[1 + \frac{1}{\hat{\eta}_c(\bar{p}_1, \bar{W}_{c1}, \bar{p}_a, \bar{T}_a)} \left(\left(\tfrac{\bar{p}_1}{\bar{p}_a} \right)^{\frac{\kappa-1}{\kappa}} - 1 \right) (1 - \eta_i) \right] \\ &= \bar{T}_a \bar{\gamma}_{Ti}(\bar{p}_1, \bar{W}_{c1}, \eta_i, \bar{p}_a, \bar{T}_a), \end{aligned} \tag{51}$$

where $\bar{p}_a$ and $\bar{T}_a$ can be measured with a low bandwidth devices or assumed constant.

Since the compressor efficiency, η_c, varies little along the steady state operating point $(\frac{p_1}{p_a}, \omega_{tc})_{ss}$ it can be treated as a constant. Consequently, $\bar{\gamma}_{Ti}$ becomes a function of only the pressure ratio across the compressor and the estimated intercooler efficiency $\hat{\gamma}_{Ti}(\bar{p}_1, \eta_{ic})$ if p_a and T_a are assumed constant. This is acceptable for $(\frac{p_1}{p_a}, \omega_{tc})_{ss}$ close to steady state, but transient deviations cause perturbations in η_c especially for $(\frac{p_1}{p_a}, \omega_{tc})$ close to the surge region. See Figure 8 for a comparison between the actual γ_{Ti}, the constructed $\bar{\gamma}_{Ti}(\bar{p}_1, \bar{W}_{c1}, \eta_{ic}, \bar{p}_a, \bar{T}_a)$ and the approximated $\hat{\gamma}_{Ti}(\bar{p}_1, \eta_{ic})$ for a large positive fueling step.

These approximations suffer from the general uncertainty in modeling compressor behavior, and should be considered only as the best currently available alternative to treating T_i constant or equal to T_1.

B Proof of Theorem

B.1 Preliminaries to the proofs

The state, $x^T := [p_1, m_1]$, is for physical reasons upper and lower bounded so that $x \in \mathcal{P}_1 \times \mathcal{M}_1 = \mathcal{D} \subset \mathbb{R}^2_+$. Since T_1 is related to p_1 and m_1 through (3) we can also assume $T_1 \in \mathcal{T}_1 \subset \mathbb{R}_+$. For estimation purposes, the input to the model is defined as $u^T := [W_{c1}, T_i, N] \in \mathcal{U}$, where $\mathcal{U} \in \mathbb{R}^3_+$ under the assumption that there are no compressor surges. Notice that $\mathcal{D}$, $\mathcal{T}_1$ and $\mathcal{U}$ under the forgoing arguments are all compact sets. Since the

volumetric efficiency is bounded we have $\eta_v(t) \in \mathcal{S}_\eta := \{\eta_v \,|0 < \eta_{vMIN} \leq \eta_v \leq \eta_{vMAX}\}\ \forall t$ so that $\theta(t) \in \mathcal{S}_\theta(t) := \{\theta(t)|\mathcal{P}_\rho(N(t))\theta(t) \in \mathcal{S}_\eta\} \subset \mathcal{S}_\theta \subset \mathbb{R}_+\ \forall t$. From (6) $\dot{\eta}_v$ becomes:

$$\dot{\eta}_v = \frac{V_1}{V_d} \frac{W''_{1e}|_{t-\delta}^{t} \int_{t-\delta}^{t} m_1(\tau)d\tau - m|_{1t-\delta}^{t} \int_{t-\delta}^{t} W'_{1e}(\tau)d\tau}{\left(\int_{t-\delta}^{t} m_1(\tau)dt\right)^2},$$

where $\delta = 2\frac{60}{N}$. For physical reasons we know that W'_{1e} and m_1 are bounded and positive so that $\int_{t-\delta}^{t} m_1(\tau)dt > 0$ $\forall \delta > 0$ so that $\dot{\eta}_v \in \mathcal{L}_\infty$.

Notice that the Theorem can be proved without assuming $p_1 \in \mathcal{L}_\infty$. However, it is then necessary to use normalization to guarantee that ϕ is bounded. Normalization is undesirable in this application since it slows down the convergence of $\hat{\theta}(t)$. Since $\phi(t) := -[H_f \kappa k_1^2 k_3 N \mathcal{P}_\rho(N) p_1](t)$, where p_1 is the output of a dynamic system (with a considerable time constant), ϕ has no sharp transients. Moreover, p_1 is positive and bounded so there are no apparent reasons for assuming $p_1 \notin \mathcal{L}_\infty$. The prior assumptions of the proof are therefore: $p_1, \Delta p_1, \bar{W}_{c1}, \bar{T}_i, \eta_v, \dot{\eta}_v, N \in \mathcal{L}_\infty$.

B.2 Proof of Proposition 1

Note that from Eq. 35 and 36 the implementable identification error can be written as

$$\bar{\epsilon} = \epsilon - [H_{df}\Delta p_1] + [H_f G_{pN}\theta \Delta p_1] + \left[H_f G_w \widetilde{W_{c1}T_i}\right] \tag{52}$$

$$= \bar{\phi}(t)\tilde{\theta} - \left[H_s \bar{\phi}(\tau)\dot{\tilde{\theta}}(\tau)\right] - [H_{df}\Delta p_1] + [H_f G_{pN}\theta \Delta p_1] + \left[H_f G_w \widetilde{W_{c1}T_i}\right] \tag{53}$$

The rate of change of the parameter error $\tilde{\theta} = \theta - \hat{\theta}$ is then defined using Eq. 52-53 and the updating law in Eq. 38:

$$\begin{aligned}
\dot{\tilde{\theta}} &= \dot{\theta} - (P+\Gamma)\bar{\phi}\bar{\epsilon} \\
&= \dot{\theta} - (P+\Gamma)\bar{\phi}\left(\bar{\phi}(t)\tilde{\theta} - \left[H_s\bar{\phi}(\tau)\dot{\tilde{\theta}}\right] - [H_{df}\Delta p_1] + [H_f G_{pN}\theta\Delta p_1] + \left[H_f G_w\widetilde{W_{c1}T_i}\right]\right) \\
&= -(P+\Gamma)\bar{\phi}^2\tilde{\theta} + (P+\Gamma)\bar{\phi}\left(\left[H_s\bar{\phi}(\tau)\dot{\tilde{\theta}}\right] + [H_{df}\Delta p_1] - [H_f G_{pN}\theta\Delta p_1] - \left[H_f G_w\widetilde{W_{c1}T_i}\right]\right) + \dot{\theta}.
\end{aligned} \tag{54}$$

By writing the filters H_s, H_{df}, and H_f from Eq. 34, 30, 29 with a common state, we get:

$$\begin{aligned}
\dot{x}_a &= -k_\omega N x_a + \bar{\phi}\dot{\tilde{\theta}} - k_\omega N\left[(G_{pN}\theta + k_\omega N)\Delta p_1 + G_w\widetilde{W_{c1}T_i}\right] \\
\dot{\tilde{\theta}} &= -(P+\Gamma)\bar{\phi}^2\tilde{\theta} + (P+\Gamma)\bar{\phi}x_a + (P+\Gamma)\bar{\phi}k_\omega N\Delta p_1 + G_w\widetilde{W_{c1}T_i} + \dot{\theta}.
\end{aligned} \tag{55}$$

This parameter error system can be written as:

$$\begin{bmatrix} \dot{x_a} \\ \dot{\tilde{\theta}} \end{bmatrix} = \begin{bmatrix} -k_\omega N + (P+\Gamma)\bar{\phi}^2 & -(P+\Gamma)\bar{\phi}^3 \\ (P+\Gamma)\bar{\phi} & -(P+\Gamma)\bar{\phi}^2 \end{bmatrix} \begin{bmatrix} x_a \\ \tilde{\theta} \end{bmatrix} + \begin{bmatrix} -G_w & -k_\omega N(G_{pN}\theta - (P+\Gamma)\bar{\phi}^2 + k_\omega N) & \bar{\phi} \\ 0 & -k_\omega N(P+\Gamma)\bar{\phi} & 1 \end{bmatrix} \begin{bmatrix} \widetilde{W_{c1}T_i} \\ \Delta p_1 \\ \dot{\theta} \end{bmatrix}, \tag{56}$$

which is a linear time varying system of the form

$$\dot{x} = A(t)x + B(t)u, \tag{57}$$

with state $x^T = [x_a, \tilde{\theta}]$ and input $u^T = [\widetilde{W_{c1}T_i}, \Delta p_1, \dot{\theta}]$ where $A(t)$ can be written

$$A(t) = (P+\Gamma)\begin{bmatrix} -\alpha + \bar{\phi}^2 & -\bar{\phi}^3 \\ \bar{\phi} & -\bar{\phi}^2 \end{bmatrix}, \quad \alpha = \frac{k_\omega N}{P+\Gamma}.$$

To establish boundedness of x we must show that (57) is stable with a bounded input. The pointwise in time eigenvalues of $A(t) + A^T(t)$ are

$$\lambda_{A+A^T}(t) = k_\omega N\left(-1 \pm \sqrt{1 - (4\alpha^{-1} - \alpha^2)\bar{\phi}^2 + 2\alpha^{-1}\bar{\phi}^4 + \alpha^{-2}\bar{\phi}^3}\right). \tag{58}$$

Since $\bar{\phi} = -\left[H_f G_{pN}\bar{p}_1\right] = -\left[H_f \kappa k_1^2 k_3 N \mathcal{P}_\rho(N)\left(p_1 + \Delta p_1\right)\right]$ where H_f is stable and $G_{pN}\bar{p}_1 = \kappa k_1^2 k_3 N \mathcal{P}_\rho(N)\left(p_1 + \Delta p_1\right)$ is bounded we have $\bar{\phi} \in \mathcal{L}_\infty$, so there are suitable choices of k_ω, Γ and $P(t_r)$ $\forall N$ such that $\exists \lambda, \mu > 0$ which satisfy

$$\int_{t_0}^{t} \lambda_{\max(A+A^T)}(\tau)d\tau \leq -\lambda(t - t_0) + \mu \quad \forall t > t_0. \tag{59}$$

Eq. 59 shows that $A(t)$ is exponentially stable.

Now we must show that the input term $B(t)u(t)$ is bounded. The least squares gain $P(t) \leq P(t_r)$ is bounded by finiteness of the initial condition $P(t_r)$, and from prior assumptions we get that $G_{pN}\theta = \kappa k_1^2 k_3 N \mathcal{P}_\rho(N)\theta = \kappa k_1^2 k_3 N \eta_v$, $\bar{\phi}$ and N are all bounded independent of t, so that $B(t)$ is uniformly bounded. Notice that

$$\dot{\theta} = \frac{d}{dt}\left(\mathcal{P}_\rho(N)\eta_v\right) = \frac{\partial \mathcal{P}_\rho(N)}{\partial N}\frac{dN}{dt}\eta_v + \mathcal{P}_\rho(N)\dot{\eta}_v \in \mathcal{L}_\infty$$

since $\mathcal{P}_\rho(N)$ is a polynomial on a compact set $N \in \mathcal{N}$, and $\dot{N}$,$\eta_v, \dot{\eta}_v \in \mathcal{L}_\infty$. From the prior assumptions to the proof $\widetilde{W_{c1}T_i}$, $\Delta p_1 \in \mathcal{L}_\infty$, and we have that $u(t)$ is bounded and conclude that $\tilde{\theta} \in \mathcal{L}_\infty$.

It remains to show that $\tilde{p}_1, \tilde{m}_1 \in \mathcal{L}_\infty$. The error dynamics of $\tilde{p}_1 = p_1 - \hat{p}_1$ are given by

$$\begin{aligned} \dot{\tilde{p}}_1 &= -g_{p1}\tilde{p}_1 - \kappa k_1^2 k_3 N \mathcal{P}_\rho(N) p_1 \tilde{\theta} \\ &\quad + \kappa k_1^2 \widetilde{W_{c1}T_i} + \kappa k_1^2 k_3 N \mathcal{P}_\rho(N) \Delta p_1 \hat{\theta} - g_{p1}\Delta p_1 \\ \hat{p}_1(t_0) &\in \mathcal{P}_1, \end{aligned} \tag{60}$$

and can be represented by the stable, operator $H_{\tilde{p}1}$.as

$$\tilde{p}_1 = \left[H_{\tilde{p}1} u_{p1}(\tau)\right](t) + \varepsilon_i(\tilde{p}_1(t_o)), \tag{61}$$

$$u_{p1}(t) = \left[-\kappa k_1^2 k_3 N \mathcal{P}_\rho(N) p_1 \tilde{\theta} + \kappa k_1^2 \widetilde{W_{c1}T_i} + \kappa k_1^2 k_3 N \mathcal{P}_\rho(N) \Delta p_1 \hat{\theta} - g_{p1}\Delta p_1\right](t), \tag{62}$$

where $\varepsilon_i(\tilde{p}_1(t_o))$ is the zero input response of (60). Since all signals in u_{p1} are uniformly bounded, we have that $u_{p1} \in \mathcal{L}_\infty$, and from $p_1(t_0), \hat{p}_1(t_0) \in \mathcal{P}_1$ we get that $\tilde{p}_1 \in \mathcal{L}_\infty$.

The error dynamics of m_1 defined as $\tilde{m}_1 = m_1 - \hat{m}_1$ are given by

$$\dot{\tilde{m}}_1 = -k_1^2 k_3 N \mathcal{P}_\rho(N)\, \hat{\theta} \tilde{m}_1 - k_1^2 k_3 N \mathcal{P}_\rho(N)\, m_1 \tilde{\theta} + \tilde{W}_{c1}, \tag{63}$$

and are exponentially stable since $-k_1^2 k_3 N \mathcal{P}_\rho(N)\, \hat{\theta} \leq -k_1^2 k_3 N \eta_{vMIN} < 0 \ \forall t$. Since $m_1 \in \mathcal{M}_1 \ \forall t$, and $\hat{m}_1(t_0) \in \mathcal{M}_1$ and we have shown that $\tilde{\theta}$ is bounded, we have that the input term $k_1^2 k_3 N \mathcal{P}_\rho(N)\, m_1 \tilde{\theta} \in \mathcal{L}_\infty$, so we can conclude that $\tilde{m}_1 \in \mathcal{L}_\infty$ which completes the proof of proposition 1

B.3 Proof of proposition 2

We will now show that $\tilde{W}_{1e} \to 0$ exponentially under Condition 1 and 2. Define the stationary solutions to (12) and (13) as

$$p_{1S} = \frac{W_{c1}T_i}{k_3 N \mathcal{P}_\rho(N)\,\theta}, \quad m_{1S} = \frac{W_{c1}}{k_1^2 k_3 N \mathcal{P}_\rho(N)\,\theta}.$$

Since Δp_1, $\tilde{W}_{c1}$ and $\dot{\theta}$ are zero and $\tilde{T}_{ic}$ is independent of time the error system (54) now becomes

$$\begin{aligned} \dot{\tilde{\theta}} &= \dot{\theta} - (P+\Gamma)\bar{\phi}\bar{\epsilon} = -(P+\Gamma)\phi\left(\epsilon + [H_{df}\Delta p_1] + [H_{df} G_{pN}\theta \Delta p_1] + \left[H_f G_w \widetilde{W_{c1}T_i}\right]\right) \\ &= -(P+\Gamma)\phi\left(\left[H_f G_{pN} p_1 \tilde{\theta}\right] + \left[H_f G_w W_{c1} \tilde{T}_i\right]\right) \end{aligned}$$

which has the stationary solution

$$\tilde{\theta}_S = \theta \frac{\tilde{T}_i}{T_i},$$

which we have established is exponentially stable in the proof of preposition 1. The error $\tilde{m}_1 = m_1 - \hat{m}_1$ given in (63) has the exponentially stable stationary solution

$$\tilde{m}_{1S} = m_{1S} \frac{\tilde{\theta}_S}{\tilde{\theta}_S - \theta}. \tag{64}$$

The air charge error, $\tilde{W}_{1e} = W_{1e} - \hat{W}_{1e}$ is

$$\tilde{W}_{1e} = k_1^2 k_3 N \mathcal{P}_\rho(N) \left(\tilde{m}_1 \left(\theta - \tilde{\theta} \right) + m_1 \tilde{\theta} \right) \tag{65}$$

and at equilibrium we have $\tilde{W}_{1e} = 0$, so that $\tilde{W}_{1e} \to 0$ exponentially.

B.4 Proof of proposition 3

Assume, $\Delta p_1, \dot{\theta}, \tilde{W}_{c1}, \tilde{T}_i$ are zero, we show that this implies that $\tilde{\theta} \to 0$ exponentially. In the proof of Proposition 1 we have established that (57) is an exponentially stable system. Since $u(t) \equiv 0$, we have that $\tilde{\theta} \to 0$ exponentially.

C Nomenclature

F_1	-	burnt gas fraction in the intake manifold
F_2	-	burnt gas fraction in the exhaust manifold
k_ω		filter coefficient
k_1	$\sqrt{\frac{\text{kJ}}{\text{m}^3 \text{ kg K}}}$	$\sqrt{\frac{R_1}{V_1}}$
k_3	$\frac{\text{m}^3 \text{ kg K}}{\text{kJ}}$	$\frac{V_d}{R_1 120}$
m_1	kg	mass of gas in the intake manifold
m_2	kg	mass of gas in the exhaust manifold
m_{ol}	kg	mass of the exhaust backflow into the cylinder during valve overlap
N	rpm	engine speed
P	-	identification gain for the least squares algorithm see Equation 39
p_1	kPa	pressure in the intake manifold
p_2	kPa	pressure in the exhaust manifold
p_a	kPa	ambient pressure
p_{cy}	kPa	in-cylinder pressure
R_1	kJ/(kg K)	gas constant for the intake manifold
r	-	engine compression ratio
T_1	K	temperature of gas in the intake manifold
T_2	K	temperature of gas in the exhaust manifold
T_a	K	ambient temperature
T_c	K	Temperature of the air leaving the compressor
T_e	K	temperature of the gas from the engine
T_{ec}	K	temperature of gas leaving the EGR cooler
T_i	K	temperature of the gas leaving the intercooler
V_1	m^3	volume of the intake manifold
V_c	m^3	instantaneous cylinder volume
V_d	m^3	total cylinder displacement volume
W_{1e}	kg/s	mass flow into the engine
W_{1eAIR}	kg/s	mass flow of fresh air into the engine

α		see Equation (8)
Γ	-	identification gain for the gradient algorithm see Equation 38
γ_{cm}	-	compressor mass flow parameter
Δp_1	kPa	unmodeled dynamics in the pressure of intake manifold
ΔT	K	mean temperature rise of the intake gas during the intake stroke
ϵ and $\bar{\epsilon}$		identification error and implementable identification error
ε_s		swapping error see Equation 33
η_c	-	compressor mechanical and isentropic efficiency
η_i	-	efficiency of the intercooler
η_v	-	volumetric efficiency of the engine
κ	-	ratio of specific heats
ϕ and $\bar{\phi}$		regressor signal and implementable regressor signal
ω_{tc}	rpm	turbocharger speed

References

[1] Guzzella L. and Amstutz A. Control of diesel engines. *IEEE Control Systems Magazine*, 18(2):53–71, 1998.

[2] Kolmanovsky I.V., Sun J., and Druzhinina M. Charge control for direct injection spark ignition diesel engines with EGR. *Proc. of the 2000 American Control Conference*, 1:34–8, 2000.

[3] Amstutz A. and Del Re L.R. EGO sensor based robust output control of EGR in diesel engines. *IEEE Transactions on Control System Technology*, 3(1):39–48, 1995.

[4] Diop S., Moral P.E., Kolmanovsky I.V., and van Nieuwstadt M. Intake oxygen concentration estimation for DI diesel engines. *Proc. of the 1999 IEEE International Conference on Control Applications*, 1:852–7, 1999.

[5] Kolmanovsky I.V., Jankovic M., van Nieuwstadt M., and Moraal P.E. Method of estimating mass airflow in turbocharged engines having exhaust gas recirculation. U.S. Patent 6,035,639, 2000.

[6] Stotsky A. and Kolmanovsky I.V. Simple unknown input estimation techniques for automotive applications. *Proc. of the 2001 American Control Conference*, 5:3312–17, 2001.

[7] Stotsky A. and Kolmanovsky I.V. Application of input estimation techniques to charge estimation in automotive engines. *IFAC Journal of Control Engineering Practice*, 10:1371–83, Dec 2002.

[8] Andersson P. and Eriksson L. Air-to-cylinder observer on a turbocharged si-engine with wastegate. SAE Technical Paper 2001-01-0262, 2001.

[9] Kolmanovsky I.V., Moral P.E., van Nieuwstadt M., and Stefanopoulou A.G. Issues in modelling and control of intake flow in variable geometry turbocharged engines. *Proc. of the 18th IFIP Conf. on System Modelling and Optimization*, 1:436–45, July 1998.

[10] Stefanopoulou A.G., Kolmanovsky I.V., and Freudenberg J.S. Control of a variable geometry turbocharged diesel engine for reduced emissions. *IEEE Transactions on Control Sytems Technology*, 8(4):733–45, 2000.

[11] van Nieuwstadt M., Kolmanovsky I.V., Moraal P.E., Stefanopoulou A.G., and Jankovic M. EGR-VGT Control Schemes: Experimental comparison for a high-speed diesel engine. *IEEE, Control System Magazine*, 20(3):63–79, June 2000.

[12] Heywood J.B. *Internal Combustion Engine Fundamentals*. McGraw-Hill, New York, 1988.

[13] Hendricks E. and Sorenson S.C. Mean value modeling of spark ignition engines. SAE Technical Paper 900616, 1990.

[14] Hendricks E. Mean value modelling of large turbocharged two-stroke diesel engine. SAE Technical Paper 890564, 1989.

[15] Taylor C.F. *The Internal-Combustion Engine in Theory and Practice*. M.I.T. Press, Cambridge, Massachusetts, 1985.

[16] C. R. Ferguson. *Internal Combustion Engines*. Wiley, New York, 1986.

[17] Hendricks E., Chevalier A., Jensen M., and Sorenson S.C. Modeling of the intake manifold filling dynamics. SAE Technical Paper 960037, 1996.

[18] Watson I. and Janota M. S. *Turbocharging the Internal Combustion Engine*. Wiley, New York, 1982.

[19] Yuen W.W. and Servati H. A mathematical engine model including the effect of engine emissions. SAE Technical Paper 840036, 1984.

[20] Grizzle J.W., Cook J.A., and Milam W.P. Improved cylinder air charge estimation for transient air-to-fuel ratio control. *Proc. of the 1994 American Control Conference*, 2:1568–73, 1994.

[21] Storset O.F., Stefanopoulou A.G., and Smith R. Air charge estimation for turbocharged diesel engines. *Proc. of the 2000 American Control Conference*, 1:28–30, 2000.

[22] Hermann R. and Krener A.J. Nonlinear controllability and observability. *IEEE Trans. on Automatic Control*, 22:728–740, 1977.

[23] Nijmeijer H. and van der Schaft A.J. *Nonlinear Dynamical Control Systems*. Springer Verlag, New York, 1996.

[24] Ioannou P.A. and Kokotovic P.V. Instabillity analysis and improvement of robustness of adaptive control. *Automatica*, 20(3):583–594, 1984.

[25] Morse A.S. Global stability of parameter adaptive control systems. *IEEE Transactions on Automatic Control*, 25:433–439, 1980.

[26] Ioannou P.A. and Sun J. *Robust Adaptive Control*. Prentice Hall, New Jersey, 1996.

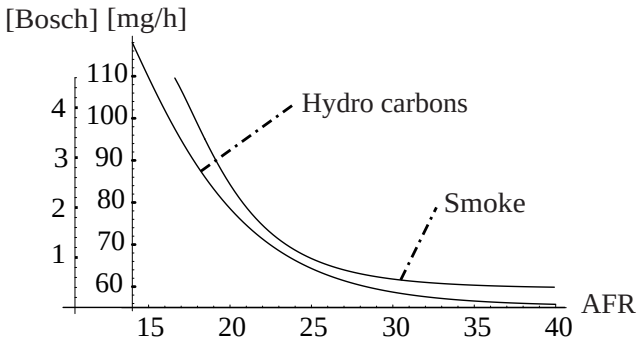

Figure 1: *Typical exhaust emissions of hydro carbons (in mg/h) and smoke (in Bosch) for diesel engines versus air-to-fuel ratio (AFR). The engine speed is 2500 rpm, and the fueling level is 6 kg/h.*

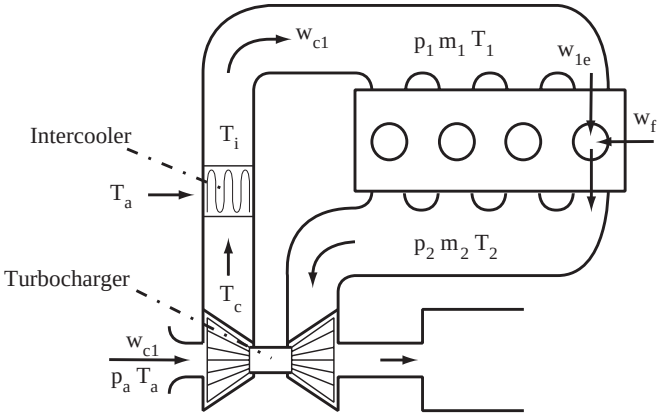

Figure 2: *A turbocharged diesel engine with intercooler*

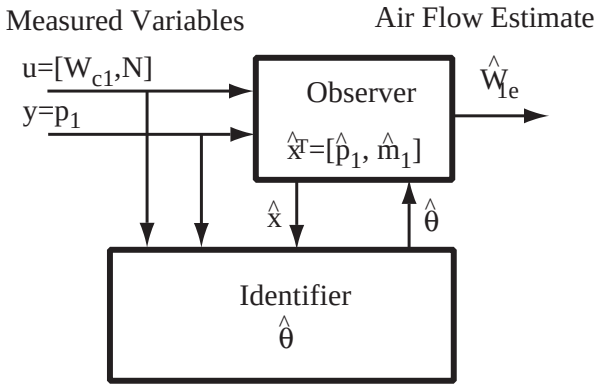

Figure 3: *Block diagram of observer and identifier where the measurement of the input to the system (12-13) is u, and the measurement of the system output is y.*

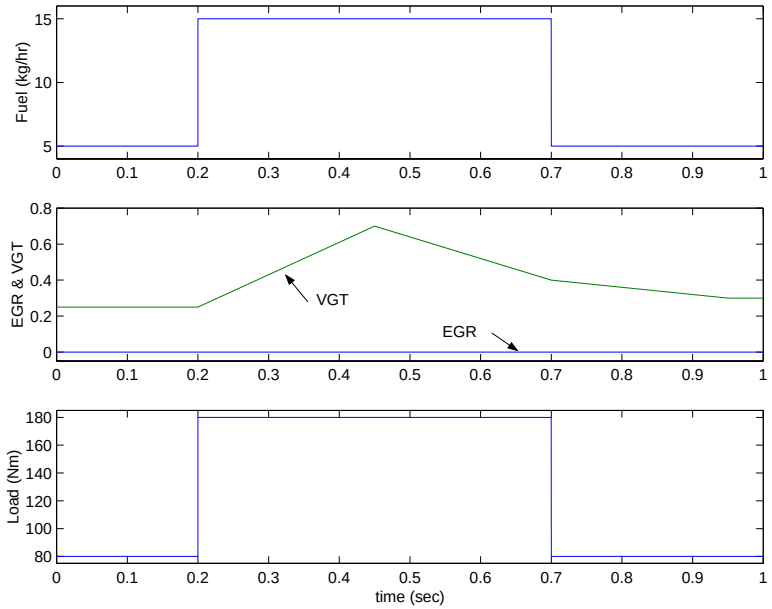

Figure 4: *Inputs to the mean-value engine model*

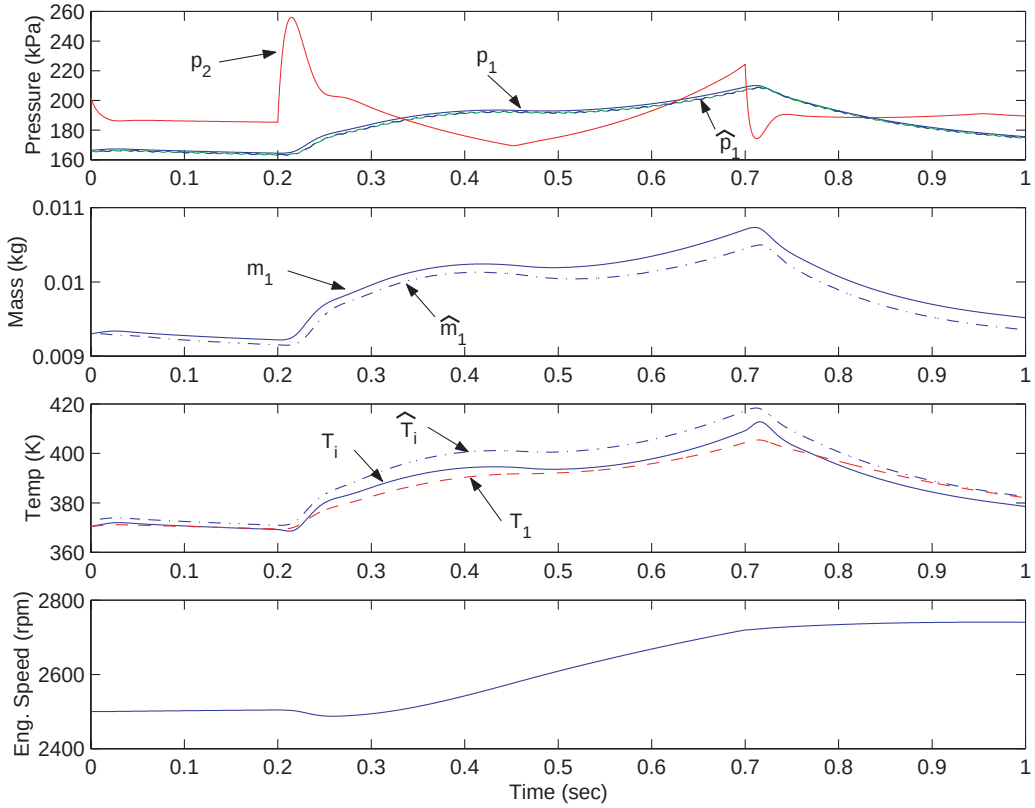

Figure 5: *States and estimated engine states*

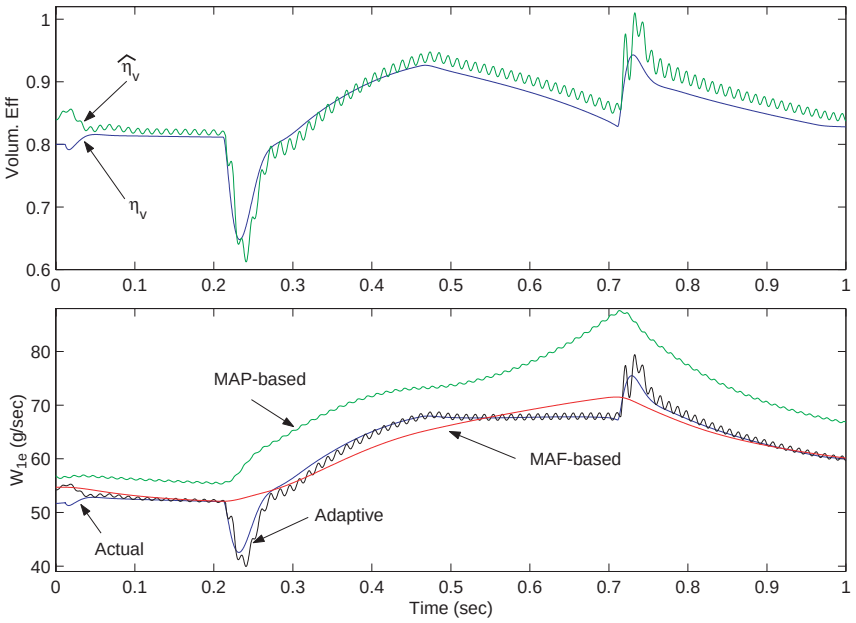

Figure 6: *Engine air flow and volumetric efficiency for the adaptive observer, speed density and mass air flow schemes.*

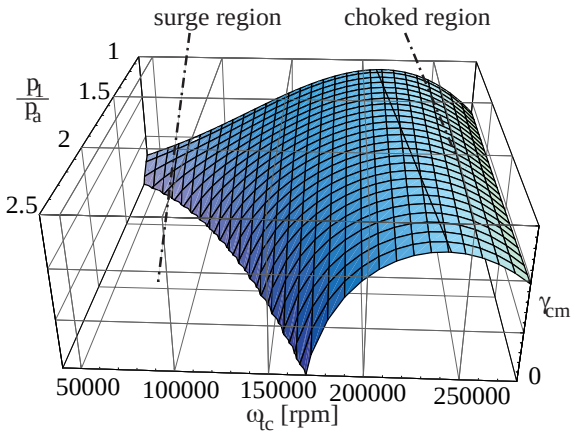

Figure 7: *Typical curve fit of compressor mass flow parameter,* γ_{cw}.

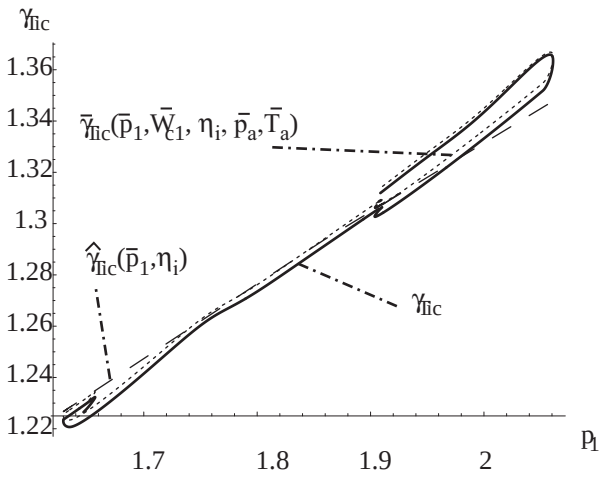

Figure 8: *Comparison of the actual γ_{Ti} and its approximations: $\bar{\gamma}_{Ti}$ and $\hat{\gamma}_{Ti}$, when $\eta_{ic} = 0$. Notice that the trajectory is generated by the same simulation as in figure 6.*

Contents

List of Figures